Co-treatment of converter slag and pyrrhotite tailings via high pressure oxidative leaching

Ilya Perederiy [a], Vladimiros G. Papangelakis [a,*], Mohamed Buarzaiga [b], Indje Mihaylov [b]

[a] Department of Chemical Engineering and Applied Chemistry, University of Toronto, 200 College Street, Toronto, ON, Canada M5S 3E5
[b] Vale, Base Metals Technology Development, 2101 Hadwen Road, Mississauga, Ontario, Canada L5K 2L3

ABSTRACT

High pressure oxidative acid leaching (HPOXAL) was successfully applied to slow-cooled converter slags from Vale's operations in Sudbury (Ontario, Canada). Extractions of Ni, Co and Cu exceeded 90% within 15–20 min and levelled at 95–97% after 45 min at 250 °C, 90 psi O_2 overpressure and 70 g/L initial H_2SO_4. Pyrrhotite tailings with ∼0.6% Ni content were also tested as a source of sulphuric acid in high pressure oxidation. Co-leaching of pyrrhotite tailings with converter slags at the same temperature, oxygen partial pressure and equivalent stoichiometric H_2SO_4 was found to have kinetics similar to that of leaching with sulphuric acid. Lowering the addition of pyrrhotite tailings (and hence, the acidity) was found to have a detrimental effect on the kinetics of leaching and final extractions (especially at 250 °C), and cause precipitation of metal sulphates. Continuous on-line acidity measurements were facilitated in experiments with an electrodeless conductivity sensor. It was shown that acid plays a major role in the conversion of fayalite to hematite and silica, and the dissolution of the base metals, while oxygen overpressure (or dispersion efficiency) determines the rate of acid generation and re-generation.

© 2011 Elsevier B.V. All rights reserved.
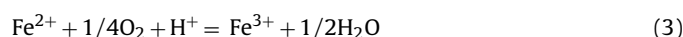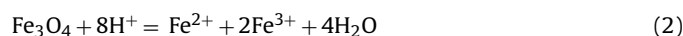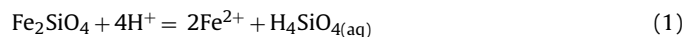
1. Introduction

High pressure oxidative acid leaching (HPOXAL) was previously applied to extract the entrapped base metals from naturally cooled (as opposed to granulated) discard smelter slags [1–4]. The process was shown to be highly versatile with fast leaching kinetics and virtually complete base metal extractions in 25–45 min at 250 °C. A slag characterization study revealed that there is little association of nickel with sulphides in the discarded flash furnace slag tested [4], which suggests that Ni tends to remain inside the oxide-silicate phase, rendering mineral flotation techniques ineffective. As a result, in order to extract nickel (as well as other oxidized base metals such as cobalt), it is necessary to facilitate the complete dissolution of the fayalite matrix, which poses no difficulty with a 0.7 M solution of sulphuric acid (∼0.2 kg of acid per kg of slag at 25% solids in the slurry) and oxygen at temperatures ranging from 200 to 250 °C.

Unlike furnace slags, converter slags are typically re-processed due to their high base metals content. At Vale's smelter operations in Sudbury (Ontario, Canada), the molten converter slags are recycled back into the flash furnaces. Such recycling decreases the new feed throughput of the smelting furnace and affects process sta-

bility. It also results in the accumulation of undesirable impurities, which end up in the converter matte – the final product of pyrometallurgical operations. In addition, recycling may cause extra fugitive emissions of sulphur dioxide from the smelting furnace to the atmosphere. Last, but not least, pyrometallurgical processing of converter slags does not favour cobalt recovery.

For the reasons mentioned above, it was interesting to test HPOXAL as a substitute technology for the recovery of base metals from converter slags. Experiments with a converter slag from Vale's smelting operations in Sudbury were conducted under conditions similar to those used with a flash furnace slag. The preliminary results, reported in conference proceedings [5], show that HPOXAL performs equally well with converter slags: extractions of ∼97% for Ni, Co and Cu were achieved within 25–45 min at 250 °C.

Previous work on slag HPOXAL [2–5] has outlined process chemistry based on the kinetic profiles of acid and iron concentrations. The following reactions were assumed to take place, as reported by Perederiy et al. [5]:

$$Fe_2SiO_4 + 4H^+ = 2Fe^{2+} + H_4SiO_{4(aq)} \tag{1}$$

$$Fe_3O_4 + 8H^+ = Fe^{2+} + 2Fe^{3+} + 4H_2O \tag{2}$$

$$Fe^{2+} + 1/4O_2 + H^+ = Fe^{3+} + 1/2H_2O \tag{3}$$

$$2Fe^{3+} + 3H_2O = Fe_2O_3 + 6H^+ \tag{4}$$

Fayalite and magnetite are dissolved by sulphuric acid, releasing ferrous and ferric iron into the solution (Eqs. (1) and (2)). Ferrous

* Corresponding author. Tel.: +1 416 978 1093; fax: +1 416 978 8605.
E-mail address: vladimiros.papangelakis@utoronto.ca (V.G. Papangelakis).

iron is then oxidized (Eq. (3)), and ferric iron is hydrolyzed (Eq. (4)) regenerating acid.

Compared to atmospheric leaching [6,7], HPOXAL requires significantly less sulphuric acid due to acid regeneration via reactions (3) and (4). It was found that an acid addition of only 20 wt% of slag weight is needed [3,5], while a minimum of 175 wt% would be required stoichiometrically according to reactions 1 and 2 in atmospheric leaching (without acid regeneration). Yet, even a 20% addition of sulphuric acid may have a detrimental effect on the process economics. The issue of operating costs in HPOXAL is further aggravated if the heat balance is taken into consideration. Operation at 250 °C would require multi-stage steam recycling as well as an additional source of heat. These concerns provide an incentive to seek a cheaper substitution for sulphuric acid as well as an alternative source of heat.

It has been reported in the past [8–11] that it is possible to produce sulphuric acid (and heat) from iron sulphide compounds such as pyrite (FeS_2) or pyrrhotite (Fe_7S_8) in situ. The following overall stoichiometric reaction holds for pyrrhotite:

$$Fe_7S_8 + 17.25O_2 + 8H_2O = 3.5Fe_2O_3 + 8H_2SO_4 \qquad (5)$$
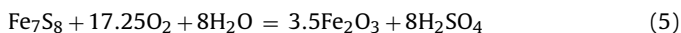
Ferron and Fleming [11] reported on the co-treatment of limonitic laterites with sulphur bearing materials (including pyrrhotite flotation tailings) in a pressure oxidative process under conditions similar to those in HPOXAL. In this work we chose to test pyrrhotite tailings (a reject stream from pentlandite ore separation by flotation) from Vale's Clarabelle Mill in Sudbury as an acid source material in converter slag HPOXAL.

Highly reactive pyrrhotite in the tailings can cause acid mine drainage due to weathering [12], which complicates containment of impounded tailings. In the co-treatment of slags with tailings, pyrrhotite is converted to stable hematite which is safer for disposal. Pyrrhotite tailings also contain a small amount of nickel (0.6–1%) which can be extracted and recovered in this process.

The present study takes on from the findings obtained previously for HPOXAL of slags [3–5] and further expands the understanding of the slag leaching chemistry. In order to interpret the kinetic results accurately, solution analysis data was complemented with in situ conductivity measurements using an electrodeless sensor in some of the experiments. The conductivity measurements were then used to measure acidity online following a procedure previously established by Huang and Papangelakis [13]. Molality was converted to grams per liter (at room temperature) using an average conversion factor of $96.2\,g\,L^{-1}\,kg\,mol^{-1}$ based on the solution samples.

2. Experimental setup, procedure, chemical analysis and solids characterization

2.1. Experimental setup and procedure

Leaching experiments were conducted in a 2 L titanium autoclave from Parr Instrument Company equipped with a custom-made acid injector consisting of a stainless steel cylinder connected to an oxygen supply via a PID pressure controller. Injection of acid and subsequent feeding of oxygen was performed through a tantalum dip tube. Solution samples were collected by filtering out solids with an in situ graphite 45 μm filter and withdrawing the liquid via a water-cooled heat exchanger. The autoclave was stirred at 800 rpm by two 4-blade impellers on a shaft connected to a magnetic drive. A schematic of the experimental setup is shown in Fig. 1.

The experimental setup was retrofitted with a modified electrodeless conductivity sensor (Fig. 2) from Foxboro Inc. The sensor
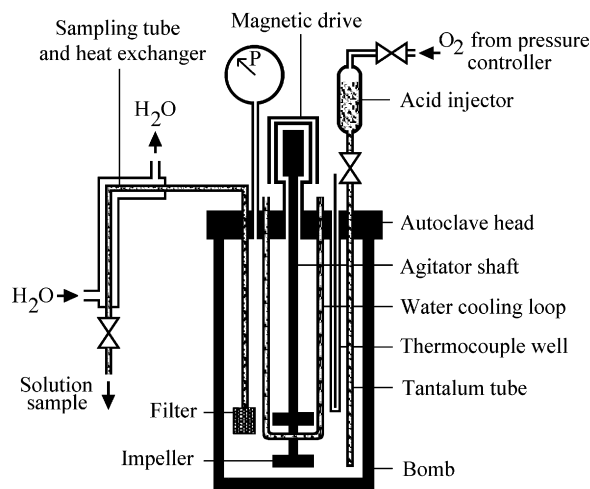

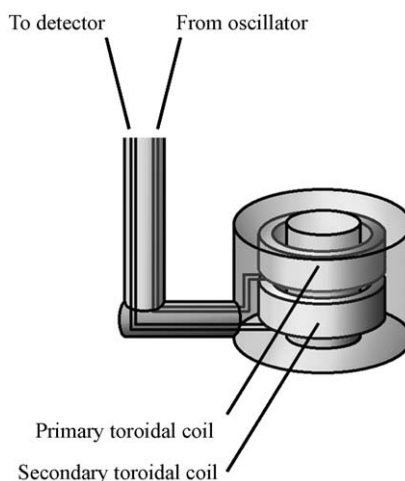**Fig. 1.** Experimental setup.

Fig. 2. Conductivity sensor.

contained two toroidal coils placed inside a glass enclosure with empty spaces filled with alumina powder [14].

Due to the sensitivity of water vapour pressure to temperature at 250 °C (±10 psi for ±1 °C), the pressure setpoint on the controller was continuously adjusted with the help of computer software based on autoclave temperature readings such that oxygen partial pressure remained with minimal oscillations. The temperature setpoint was maintained by a PID controller manipulating both electric heating and water cooling of the autoclave.

The retention time was counted from the moment of oxygen introduction into the system, which typically occurred at 20 °C below the setpoint. Due to the highly exothermic reactions taking place, the autoclave attained its target temperature within 1–2 min from the moment of oxygen (or oxygen and acid) introduction. Samples were withdrawn at intervals of 5 min or greater.

Upon test completion, the autoclave was cooled to 70 °C and depressurized. Cooling typically took ~15 min. The slurry was filtered, and the cake of the primary filtration was washed (on the filter) with 0.5 L of 5 g/L H_2SO_4 followed by 0.5 L of deionized water. The residue was then dried at ~70–80 °C in an oven for 1–3 days.

2.2. Chemical analysis and characterization of solids

Intermediate solution samples, filtrates as well as solutions after residue digestion were analyzed for metals, silicon and sulphur

Table 1
Slag assays, %wt.

Slag	Ni	Cu	Co	Zn	Fe	S	Si	Al	Ca	Mg	K	Pb	Mn	Cr
#1	1.05	0.69	0.63	0.16	52.8	0.77	12.1	0.17	0.08	0.06	0.04	0.04	0.02	0.02
#2	1.07	0.68	0.67	0.15	52.5	0.76	12.7	0.20	0.09	0.07	0.08	0.07	0.02	0.01

Table 2
Pyrrhotite tailings assay, %wt.

Ni	Cu	Co	Zn	Fe	S	Si	Al	Ca	Mg	K	Ti	Mn	Cr
0.595	0.086	0.021	0.020	39.1	21.4	8.49	2.39	1.45	0.995	0.425	0.253	0.06	0.03

using Inductively Coupled Plasma-Optical Emission Spectroscopy (ICP-OES). All concentrations reported are based on solution volume at 25 °C. The extractions "at temperature" reported in this work are calculated according to Eq. (6). The denominator of the fraction changes in each test to represent the total amount of metal (and sulphur) loaded into the autoclave with the feed materials.

$$\alpha_i = \frac{\sum_{j=1}^{i} c_j V_j + c_i(\hat{V} - \sum_{j=1}^{i} V_j)}{\sum_{j=1}^{N} c_j V_j + c_F V_F + c_W V_W + X_m \cdot m_R} \cdot 100 \qquad (6)$$

c_i, c_j, are the concentrations in the i-th and j-th (of N) samples [g/L], V_j is the volume of the j-th sample [L], $\hat{V}$ is the initial volume of solution inside the autoclave (based on room temperature) [L], c_F, c_W are the concentrations in the primary and wash filtrates [g/L], V_F, V_W are the volumes of the primary and wash filtrates [L], X_m, m_R are the metal (and sulphur) mass fraction in the residue and the mass of the residue [g/g, g].

Typically, the difference between the extractions calculated according to Eq. (6) and extractions calculated according to the modified equation that uses an average element concentration in the feed, as explained above, was ~3%. Free sulphuric acid in solutions was determined by titration with NaOH in the presence of CaCDTA as a masking agent. Fe(II) was determined by express-titration with $KMnO_4$ and verified with $K_2Cr_2O_7$ for select samples.

The particle size distributions of the feed materials were determined using a light scattering technique with a Malvern Mastersizer S instrument. Scanning Electron Microscopy (SEM) images of slag were obtained on a JEOL JSM-840 scanning electron microscope utilizing back-scattered electrons (BSE) at 15 keV accelerating potential difference.

3. Feed materials

3.1. Converter slag

Converting of furnace mattes in Pierce-Smith converters (a batch process with poor settling characteristics) results in the production of slags with highly variable content of base metals and magnetite. The two converter slag samples used in this work were similar to those typically produced in the beginning of a converting process, when elevated levels of magnetite are present. The ratio of magnetite to fayalite determined with Rietveld refinement at the University of British Columbia from powder X-ray diffractograms was ~1:4 (by weight). Both slags were found to be similar in terms of their chemical compositions (Table 1), and indistinguishable in terms of microstructure, as revealed by SEM-BSE.

An SEM-BSE cross-section image of a typical slag particle (Slag #2) is shown in Fig. 3. Four mineral phases were identified with the help of EDX spectra: fayalite, magnetite, silica and mixed matte. Area A in Fig. 3 represents fayalite, the mesh-like structure of which suggests that it contained dissolved silica, which segregated during solidification. Matte appeared in the form of entrapped droplets in area B and in several other bright spots. Ni:Cu:Fe ratios in matte
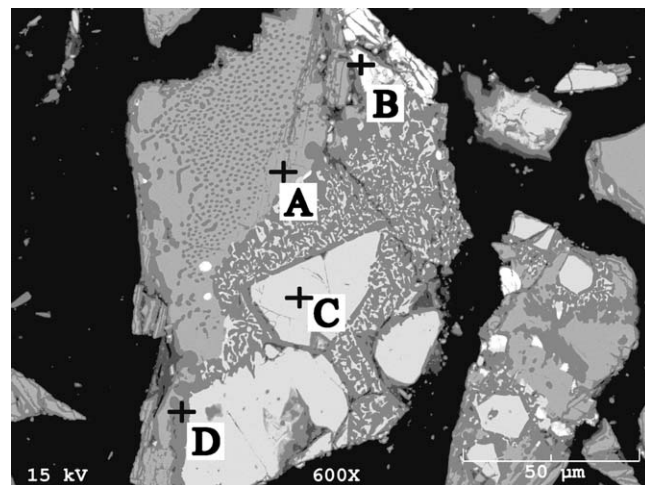

Fig. 3. Cross-section SEM-BSE image of typical converter slag particles.

particles were found to be highly variable from particle to particle, with Cu-Fe matte being more abundant than Ni–Fe matte. Magnetite usually appeared as large chunks (area C) as well as small inclusions in silica (around area C). Silica usually surrounded fayalite and magnetite such as in area D.

Copper and nickel were encountered within matte inclusions, although in rare cases small peaks for nickel were also seen on EDX spectra for fayalite and magnetite. Cobalt was never observed due to its high dispersion in the silicate-oxide phases as well as overlapping of its Kα spectral lines with those of iron.

Overall, the mineralogy of the converter slags used in this work is similar to the flash furnace slag described previously [4], although the ratio of the constituting minerals is different.

The particle size distribution of the converter slags (shown in Fig. 4) was chosen such as to ensure that all particles could be suspended by stirring, keeping the grinding to the minimum.

3.2. Pyrrhotite tailings

Pyrrhotite tailings from Vale's Clarabelle Mill were used in this work as a replacement for sulphuric acid. The assay is shown in Table 2.

The tailings sample used in this work was dried at 70 °C; as a result, the originally fine material became clumped. In order to return the material into its original state, it was passed through a roller crusher such that re-grinding was avoided. The particle size distribution for the obtained material is shown in Fig. 4.
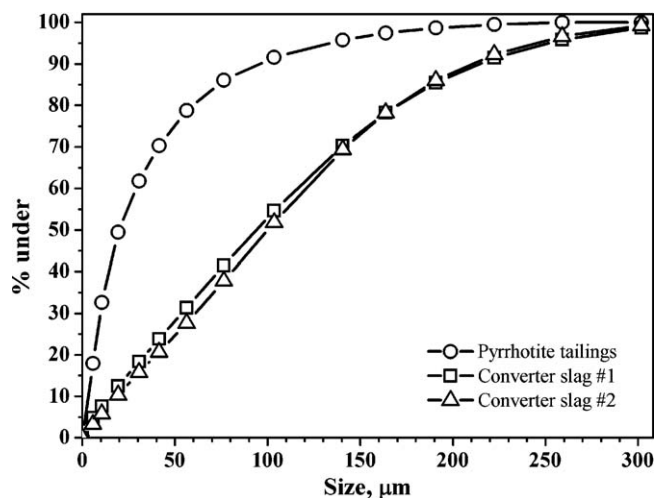
Fig. 4. Particle size distributions of pyrrhotite tailings and slags.

Powder X-ray diffraction did not detect any products of pyrrhotite oxidation in the dried tailings, and minor surface oxidation is not believed to introduce any significant bias into the assessment of the acid generation capacity of the tailings.

4. Results and discussion

4.1. Sulphuric acid injection

Three experiments with injected sulphuric acid were conducted to obtain kinetic curves for the baseline conditions ($250\,^\circ$C, 70 g/L initial H_2SO_4 based on room temperature volume, 25% solids, 90 psi O_2). These results, presented in Fig. 5, can be used to compare the behaviour of the two converter slag feeds and determine the reproducibility of the tests. The maximum standard deviation of metal extractions at temperature is ~5%; whereas the maximum standard deviation of final extractions (i.e., those estimated after cooling) is under 1%. As can be seen from the figures, extractions of Ni, Co and Cu achieve 90% within 15–20 min after acid injection and oxygen introduction. Both feeds exhibited comparable kinetics, which complements the assays and SEM characterization in proving the similarity of the two feeds.

The bulk of the sulphuric acid injected enters the autoclave instantaneously; therefore the decreased acidity (29–37 g/L) in 5 min (Fig. 5d) proves that dissolution of fayalite is a very fast reaction, while acid regeneration due to Fe(II) oxidation and Fe(III) hydrolysis is a slower process. Acid is regenerated to ~75% of its initial level (70 g/L) at temperature, but cooling results in lower acidities due to the re-dissolution of the precipitated iron (III) compounds (predominantly, hematite): ~36 g/L or 52% of the initial acidity. This corresponds to the following net acid consumptions:
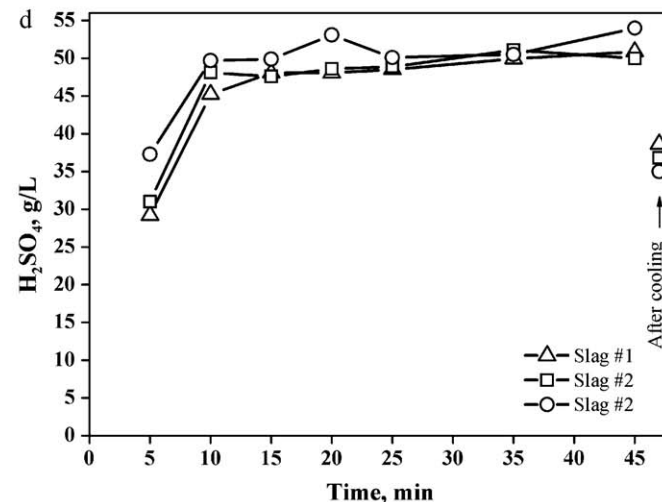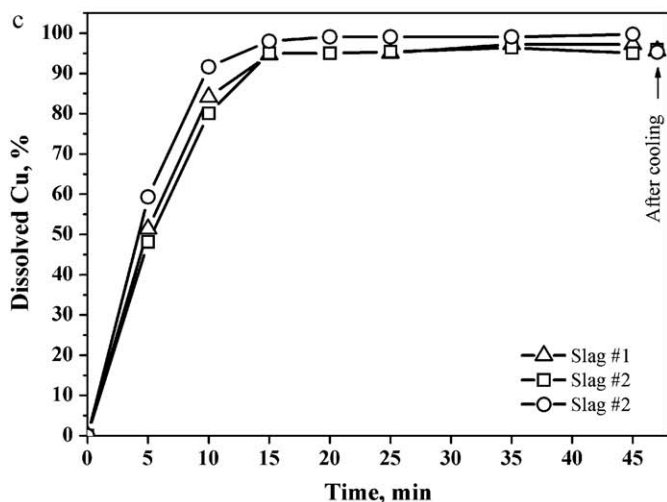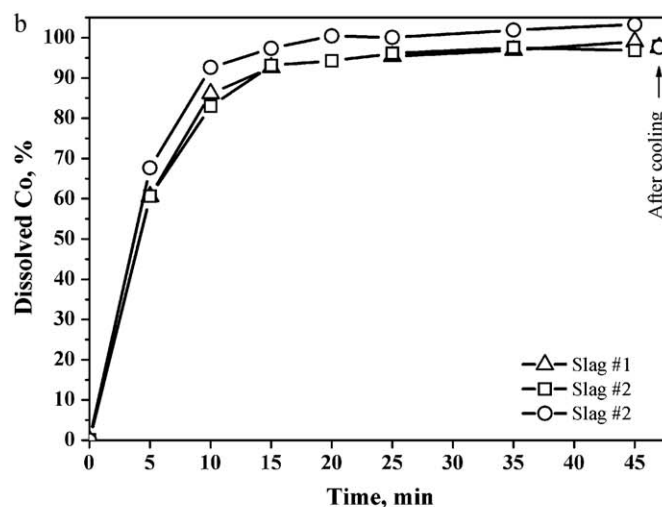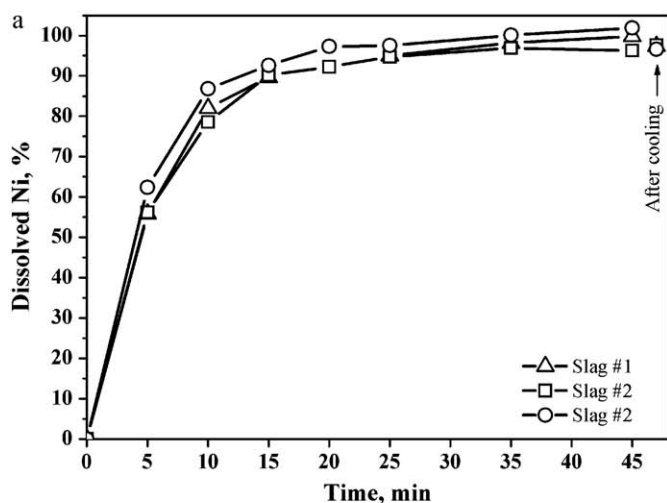

Fig. 5. Kinetics of leaching with injected H_2SO_4: $250\,^\circ$C, 70 g/L H_2SO_4, 25% solids in slurry, 90 psi O_2. Note: data after cooling is reported without reference to the actual time.
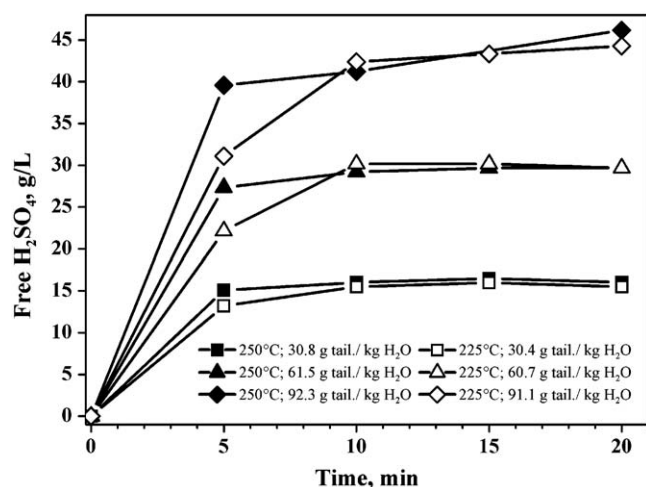
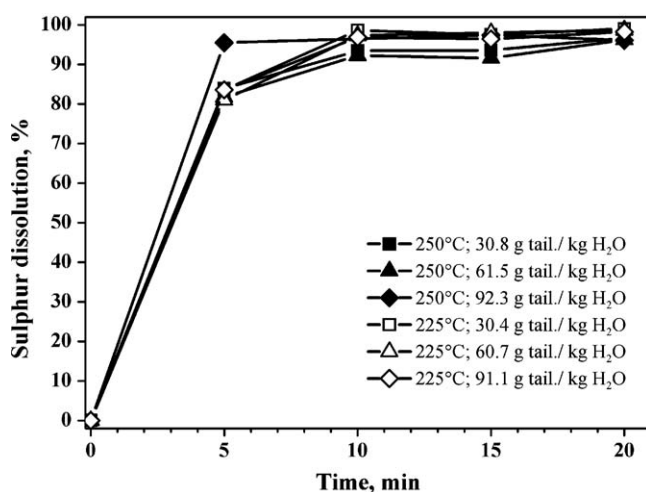Fig. 6. Acid profiles during pressure oxidation of pyrrhotite in tailings at 90 psi O_2.

Fig. 7. Sulphur dissolution during pressure oxidation of pyrrhotite in tailings at 90 psi O_2.

0.05 kg H_2SO_4/kg slag at 250 °C, and 0.1 kg H_2SO_4/kg slag after cooling and filtration.

4.2. Addition of pyrrhotite tailings

Several pressure oxidation experiments with the pyrrhotite tailings and water alone were conducted at 225° and 250 °C to evaluate the efficacy of the tailings for acid generation. Acid generation is completed in 10 min regardless of temperature (225° and 250 °C) with less than 61.5 g of tailings addition per kg of water as indicated by the acid profiles in Fig. 6. Increasing the addition of the pyrrhotite tailings prolongs acid generation. Based on sulphur dissolution profiles, pyrrhotite oxidation is virtually complete in 20 min with over 96% of sulphur dissolved (as sulphate) according to Eq. (6) – Fig. 7.

Stoichiometrically equivalent acidities (defined as the concentration of free H_2SO_4 plus the concentration of H_2SO_4 that could be obtained by hydrolyzing all the iron present in the solution–as per the reaction in Eq. (5)) after 20 min of pressure oxidation are shown in Fig. 8. The plot reveals the same linear relationship between equivalent acidity and pyrrhotite addition for both temperatures. Approximately 160 g of H_2SO_4 can be produced from 133 g of pure pyrrhotite (39.5% S), according to Eq. (5). Using the actual content of sulphur in the tailings (21.3%), and neglecting the amount of sulphur not associated with iron, Eq. (5) gives ∼87 g/L H_2SO_4 for a tailings addition of 133 g per kg of water. The experimentally
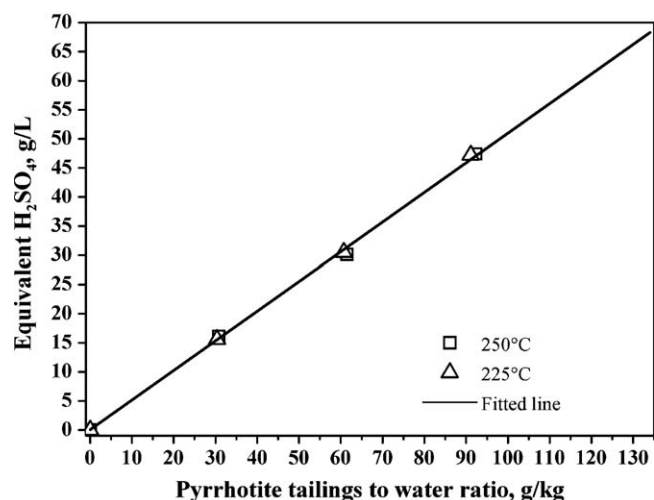

Fig. 8. Equivalent acidity from pressure oxidation of pyrrhotite in tailings at 90 psi O_2 in 20 min.

determined acidity is lower (68 g/L, or 78% efficiency) due to the dissolution of acid consuming minerals (of Al, Mg and Ca).

The equivalent acidities tested in this work are 34 and 68 g/L, and the required pyrrhotite additions are found from Fig. 8 to be 67 and 133 g/kg of water. Experiments at these acidities were conducted at 225° and 250 °C, and compared to an experiment run at 250 °C, in which acid was injected to make the initial concentration 70 g/L. The kinetic curves for Ni, Co, Cu and free acidity are shown in Fig. 9.

As is clear, only a combination of high temperature and acidity (i.e., 250 °C and ∼68 g/L) leads to extractions of Ni and Co in excess of 90% after 15–20 min of leaching (Fig. 9a and b). It is also only under these conditions that leaching is completed within 45 min (96–97% of Ni and Co extracted). At 68 g/L equivalent acidity, a decrease in temperature to 225 °C naturally results in a slower leaching rate: only 86–87% of Ni and Co are extracted in 45 min (at temperature), but extractions after cooling and filtration increase up to 92% for Ni and 95% for Co (Fig. 9a and b).

Interestingly, in experiments with 34 g/L equivalent acidity, decreasing the temperature from 250° to 225 °C improves Co extraction (from 80% to 89% in 45 min at temperature, and from 83% to 90% after cooling and filtration) as can be seen from Fig. 9b. Such behaviour can be explained by precipitation of $CoSO_4$ at 250 °C when acidity is low due to fast fayalite dissolution (Fig. 9d).

At constant free acid introduction of magnesium sulphate, a typical divalent metal sulphate, into high temperature H_2SO_4–H_2O systems results in the decrease of the concentration of H^+ due to the formation of the bisulphate ion [15]. Equilibrium is governed by the following equations:

$$MgSO_4 \cdot H_2O = Mg^{2+} + SO_4^{2-} + H_2O \tag{7}$$

$$H^+ + SO_4^{2-} = HSO_4^- \tag{8}$$
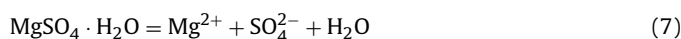
A decrease in the free acidity would increase the dissociation of the bisulphate ion in the system (Eq. (8)), which in turn would cause precipitation of magnesium sulphate (Eq. (7)). Other divalent metal sulphates are known to behave in the same manner. Modelling and experimental data [16–18] confirm that the solubility of metal sulphates such as $MgSO_4$, $NiSO_4$ and $FeSO_4$ decreases with decreasing free acidity and increasing temperature in H_2SO_4–H_2O systems at temperatures of 200 to 250 °C.

It is likely that in the experiment at 250 °C and 34 g/L equivalent acidity, $FeSO_4$, $NiSO_4$ and $CoSO_4$ precipitated during the first few minutes of the experiment, when acid was spent to dissolve slag. Precipitation of ferrous sulphate was confirmed by an increase in
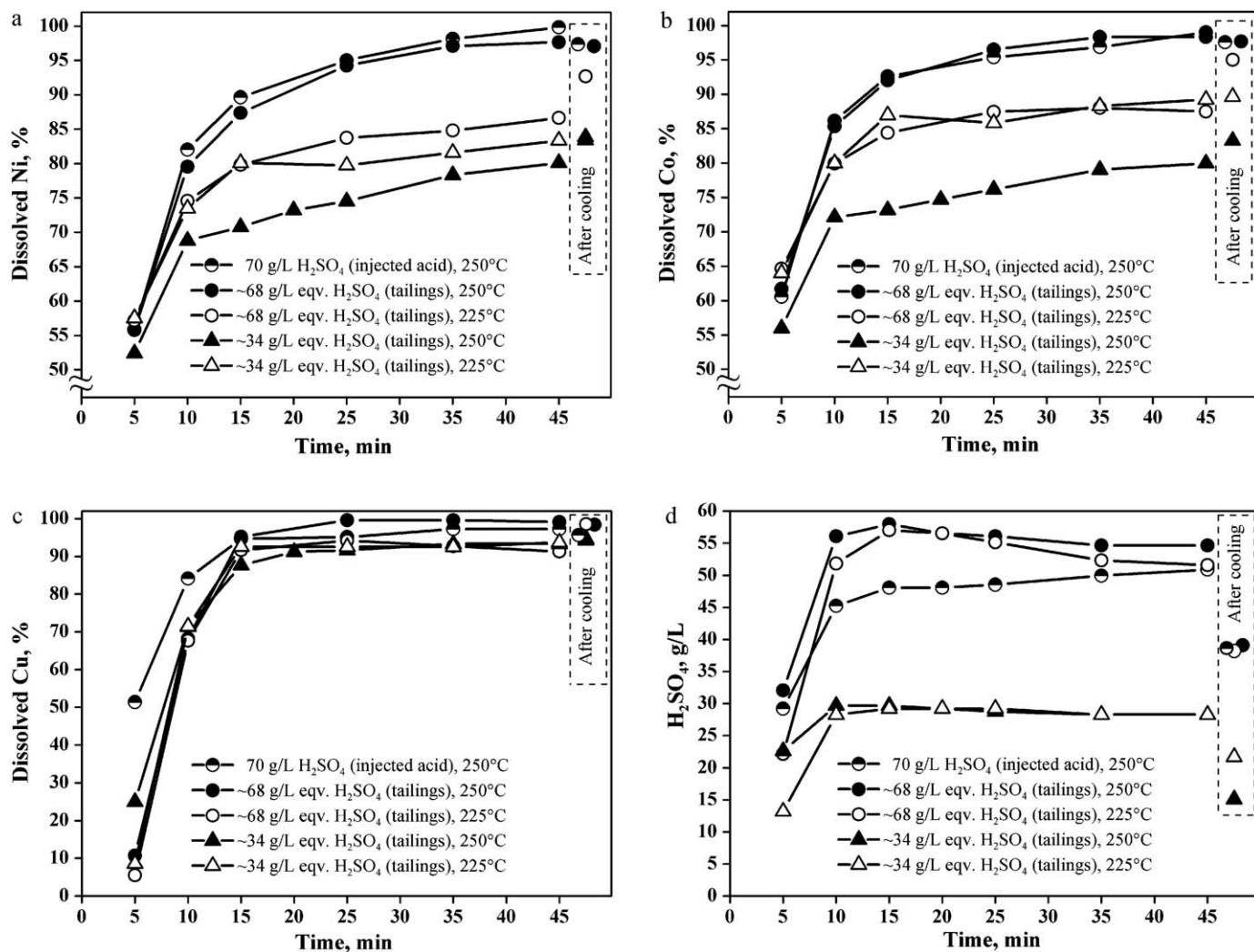
Fig. 9. Kinetics of leaching: 90 psi O_2, 25 wt% total solids (slag #1 and pyrrhotite tailings). Note: data after cooling is reported without reference to the actual time.

the concentration of ferrous iron from under 100 ppm at 250 °C to more than 1 g/L after cooling and filtration. Similarly, the concentrations of Ni and Co increased after cooling and filtration in the experiment run at 250° (34 g/L equivalent acidity), while it was not the case in the experiment run at 225 °C. It appears that precipitation of ferrous sulphate is able to slow down leaching by preventing quick acid regeneration. In an industrial process, bulk precipitation of base metal sulphates is not known as a significant scale formation contributor.

Prolonging leaching to 120 min in the experiment at 250 °C and 34 g/L equivalent acidity improves both Ni and Co extractions from 83% to approximately 92% (Fig. 10).

Copper extractions (Fig. 9c) are practically insensitive to the conditions used. Naturally, copper dissolution proceeds slower in the case of leaching with pyrrhotite tailings compared to tests with injected sulphuric acid (Fig. 9c). This is due to the fact that copper sulphide is more stable than pyrrhotite. At 250 °C, elemental sulphur formation during matte oxidation under oxygen pressure is not expected to occur [19,20].

The residues of leaching contain crystalline hematite and amorphous silica which are both inert materials and are formed under conditions similar to those employed in the High Pressure Acid Leaching process for nickeliferous laterites (e.g., the Goro Nickel Process [21]). Hence, an established disposal technology would be employed. The average residue compositions at various
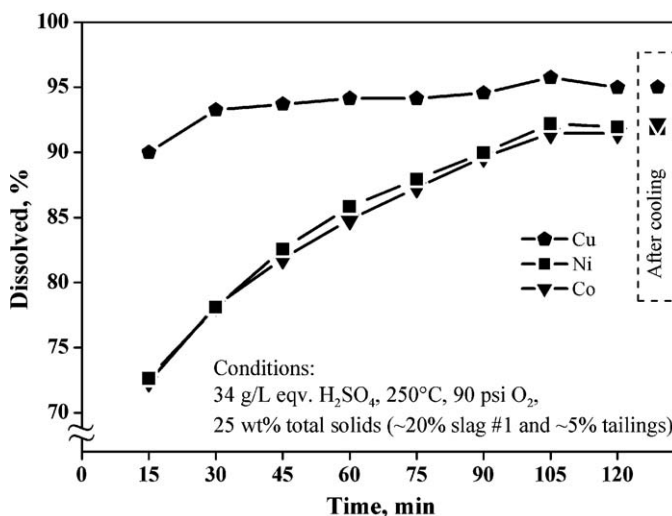

Fig. 10. Kinetics of prolonged leaching: 34 g/L eqv. H_2SO_4, 250 °C, 90 psi O_2. Note: data after cooling is reported without reference to the actual time.

Table 3
Average residue compositions, %wt. Experimental conditions: 25 wt% total solids, 90 psi O_2; 800 rpm, 45 min.

Temperature	Acidity	Ni	Co	Cu	Fe	Si	Al	Ca	Mg	S
250 °C	70 g/L	0.027	0.016	0.031	48.1	11.7	0.36	<0.05	0.01	0.96
250 °C	68 g/L (eqv.)	0.027	0.010	0.008	45.9	11.2	0.61	0.18	0.08	0.78
250 °C	34 g/L (eqv.)	0.033	0.167	0.092	47.3	11.3	0.45	0.12	0.07	0.63
225 °C	68 g/L (eqv.)	0.076	0.025	0.009	49.2	11.3	0.87	0.28	0.15	0.97
225 °C	34 g/L (eqv.)	0.149	0.056	0.034	47.4	11.1	0.66	0.16	0.09	0.72
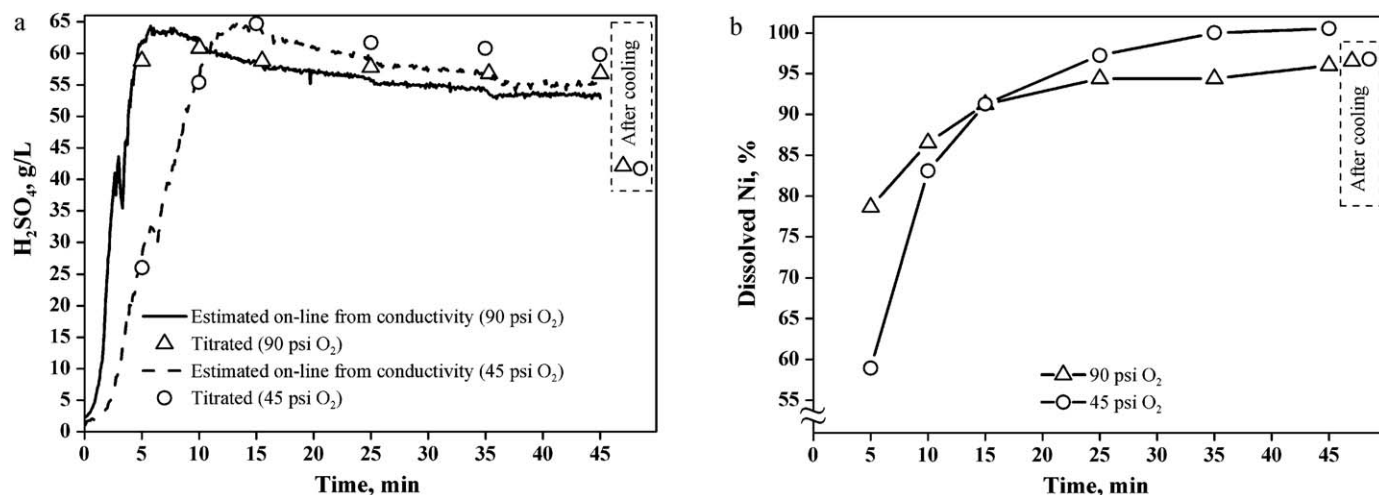
Fig. 11. On-line acid profiles and leaching kinetics: Slag #1 and pyrrhotite tailings, 250 °C, 25% total solids in slurry (including 9.75% tailings), ~68 g/L eqv. H_2SO_4.

conditions are shown in Table 3. The residues contain 0.6–1 wt% of sulphur present in the form of entrapped soluble sulphates and possibly products of partial hydrolysis such as hydronium alunite, $H_3OAl_3(SO_4)_2(OH)_6$.

Evidently, acidity plays a major role in the dissolution of fayalite and magnetite (Eqs. (1) and (2)) that leads to the release of the entrapped base metals. The effect of oxygen partial pressure on the rate of acid generation and nickel dissolution can be illustrated by two experiments run at 45 and 90 psi O_2 (Fig. 11). Continuous on-line acid measurements in these experiments were obtained from conductivity data. The average relative deviation (ARD) value between the estimated and measured acidities (calculated according to Eq. (9)) was found to be below 4.6%.

$$ARD = \frac{\Sigma |1 - c_{calc}/c_{exp}|}{N} \times 100\% \tag{9}$$

Monitoring the acidity using conductivity makes it possible to obtain information about the processes taking place during the first few minutes of the experiment, which is not possible with a conventional sampling technique. As expected, acidity builds up gradually (Fig. 11a), with the maximum build-up rate attained after an induction period of 1–2 min during which sufficient amounts of ferric iron are expected to accumulate in order to support fast hydrolysis.

Dips on the acidity curves (Fig. 11a) at ~3 and 6 min are attributed to disruption in oxygen dispersion due to pressure overshoots, which forced the controller to interrupt the flow of the gas through the dip tube allowing acid consuming reactions (mainly fayalite dissolution according to Eq. (1)) to briefly take over acid generation (Eq. (4)). The magnitude of the dips suggests high rates of fayalite dissolution.

The concentration of free acid reaches its maximum at ~7 min (at 90 psi O_2) and 13 min (at 45 psi O_2), and then decreases slowly with a tendency towards levelling off (Fig. 11a). Solution analysis shows that the concentrations of Mg and Al keep increasing until

the end of the experiment. Therefore, this decrease in acidity is attributed to the neutralization by MgO and Al_2O_3.

Although the partial pressure of oxygen (or oxygen dispersion) affects the kinetics of nickel dissolution at the early stages of leaching (Fig. 11b), extractions after 10 min (>80%) do not differ significantly in experiments with 45 and 90 psi O_2. The 5% difference in the extractions at 45 min is attributed to errors in the determination of the liquor volume in the autoclave due to steam leakage. It is possible that higher partial pressures of oxygen (or better means of gas dispersion) could further improve the kinetics of leaching; however, this was not verified due to the inability of the autoclave cooling system to avert a spike in temperature caused by extensive heat generation.

5. Summary and conclusions

High pressure oxidative acid leaching (HPOXAL) was successfully applied to slow-cooled converter slags. Extractions of Ni, Co and Cu exceeded 90% within 15–20 min and arrived at 95–97% after 45 min at 250 °C, 90 psi O_2 overpressure and 70 g/L initial H_2SO_4.

A modified high pressure oxidation process was tested in order to evaluate the performance of an iron sulphide feed as a substitute for sulphuric acid. Pyrrhotite tailings were selected for their content of Ni (~0.6%) and reactivity. The amount of equivalent acid produced was found to be a linear function of tailings addition. Pyrrhotite oxidation and iron hydrolysis were completed within ~20 min for pyrrhotite tailing additions under 92 g/kg H_2O at 250 °C, 90 psi O_2 overpressure.

Oxidative co-leaching of pyrrhotite tailings with converter slags at 250 °C, 90 psi O_2, 68 g/L equivalent H_2SO_4 (corresponding to an acid addition of ~20% of solid feed weight at 25% solids) was shown to have kinetics comparable to adding sulphuric acid with final extractions reaching 95–97% in 45 min.

An explanation was offered to the detrimental effect of high temperature (250 °C) combined with a low equivalent acidity (34 g/L–corresponding to an acid addition of ~10% of solid feed

weight at 25% solids) on the kinetics of Ni and Co dissolution. It was shown that divalent metal sulphates ($FeSO_4$, $NiSO_4$, $CoSO_4$) precipitate at low acidities.

On-line acid monitoring using conductivity in co-leaching experiments (at 250 °C, 45 and 90 psi O_2, ~68 g/L equivalent H_2SO_4) confirmed that acidity gradually builds up in the system in the first 7–13 min, with oxygen overpressure (and dispersion) determining the rate of acid generation and re-generation. It is likely that achieving oxygen overpressures above 90 psi (or better means of gas dispersion) could improve the rate of acid generation and, ultimately, base metal dissolution during the early stages of leaching.

Acknowledgements

References

[1] W. Curlook, V.G. Papangelakis, Pressure acid leaching of non-ferrous smelter slags for the recovery of their base metal values, in: M.J. Collins, V.G. Papangelakis (Eds.), Pressure Hydrometallurgy 2004 (conference proceedings), Canadian Institute of Mining Metallurgy and Petroleum, Montreal, 2004, pp. 823–837.

[2] M. Baghalha, V.G. Papangelakis, W. Curlook, Factors affecting the leachability of Ni/Co/Cu slags at high temperature, Hydrometallurgy 85 (2007) 42–52.

[3] Y. Li, I. Perederiy, V.G. Papangelakis, Cleaning of waste smelter slags and recovery of valuable metals by pressure oxidative leaching, J. Hazard. Mater. 152 (2008) 607–615.

[4] Y. Li, V.G. Papangelakis, I. Perederiy, High pressure oxidative acid leaching of nickel smelter slag: Characterization of feed and residue, Hydrometallurgy 97 (2009) 185–193.

[5] I. Perederiy, V.G. Papangelakis, C.Q. Jia, Pressure oxidative leaching of slags from nickel smelters: an update, in: J.J. Budac, R. Fraser, I. Mihaylov, V.G. Papangelakis, D.J. Robinson (Eds.), Hydrometallurgy of Nickel and Cobalt (Proceedings of 39th annual Hydrometallurgy Meeting), Canadian Institute of Mining, Metallurgy and Petroleum, Montreal, 2009, pp. 87–96.

[6] C.Q. Jia, J.Z. Xiao, R.G. Orr, Behaviour of metals in discard nickel smelter slag upon reacting with sulphuric acid, J. Environ. Sci. Health A34 (5) (1999) 1013–1034.

[7] A.N. Banza, E.G. Gock, K. Kongolo, Base metals recovery from copper smelter slag by oxidising leaching and solvent extraction, Hydrometallurgy 67 (2002) 63–69.

[8] D.C. Seidel, E.F. Fitzhugh Jr., A hydrothermal process for oxidized nickel ores, Mining Eng. (1968) 80–86, April.

[9] C.E. O'Neill, Acid leaching of lateritic ores, Canadian Patent No. 947,089, May 4, 1974.

[10] V. Opratko et al., Acid leaching of lateritic ores, U.S. Patent 3,809,549, May 7, 1974.

[11] C.J. Ferron, C.A. Fleming, Co-treatment of limonitic laterites and sulphur-bearing materials as an alternative to the HPAL process, in: W.P. Imrie (Ed.), Pressure Acid Leaching (Proceeding of the International Laterite Nickel Symposium—2004), TMS, 2004, pp. 245–261.

[12] M.C. Moncur, J.L. Jambor, C.J. Ptacek, D.W. Blowes, Mine drainage from the weathering of sulphide minerals and magnetite, Appl. Geochem. 24 (2009) 2362–2373.

[13] M. Huang, V.G. Papangelakis, Online free acidity measurement of solutions containing base metals, Can. Metall. Q. 47 (2008) 269–276.

[14] R.S. Saini, V.G. Papangelakis, On-line acid measurements via electrodeless conductivity in HPAL processes for Ni/Co extraction, in: R. Budac, I. Fraser, V.G. Mihaylov, D.J. Papangelakis, Robinson (Eds.), Hydrometallurgy of Nickel and Cobalt (Proceedings of 39th annual Hydrometallurgy Meeting), Canadian Institute of Mining Metallurgy and Petroleum, Montreal, 2009, pp. 87–96.

[15] M. Baghalha, V.G. Papangelakis, The ion–association-interaction approach as applied to aqueous H_2SO_4–$Al_2(SO_4)_3$–$MgSO_4$ solutions at 250 °C, Metall. Mater. Trans. 29B (1998) 1021–1030.

[16] J. Jankovic, V.G. Papangelakis, S.N. Lvov, Effect of nickel and magnesium sulphate on pH of sulphuric acid solutions at elevated temperatures, J. Appl. Electrochem. 39 (2009) 751–759.

[17] G. Bruhn Von, J. Gerlach, F. Pawlek, Untersuchungen über die löslichkeiten von salzen und gasen in wasser und wäβrigen losungen bei temperaturen oberhalb 100 °C, Zeitschrift für anorganische und allgemeine Chemie 337 (1965) 68–79.

[18] F. Hasegawa, K. Tozawa, T. Nishimura, Solubility of ferrous sulfate in aqueous solutions at high temperatures, Shigen to Sozai 112 (12) (1996) 879–884.

[19] J.A. King, D.B. Dreisinger, Autoclaving of copper, in: W.C. Cooper (Ed.), Electrorefining and Hydrometallurgy of Copper (Proceedings of Copper 95 International Conference), Canadian Institute of Mining Metallurgy and Petroleum, Montreal, 1995, pp. 511–533.

[20] V.G. Papangelakis, G.P. Demopoulos, Acid pressure oxidation of arsenopyrite: part I, Can. Metall. Q. 29 (1990) 1–12.

[21] Y. Okita, A. Singhal, J.-J. Perraud, Iron control the Goro Nickel process, in: J.E. in:, P.A. Dutrizac, Riveros (Eds.), Iron Control Technologies (Proceedings of the third international symposium on iron control in hydrometallurgy), Canadian Institute of Mining, Metallurgy and Petroleum, Montreal, 2006, pp. 635–651.